AJNR

Diffuse Metabolic Abnormalities in Reversible Posterior Leukoencephalopathy Syndrome

Florian S. Eichler, Paul Wang, Robert J. Wityk, Norman J. Beauchamp, Jr and Peter B. Barker

AJNR Am J Neuroradiol 2002, 23 (5) 833-837
http://www.ajnr.org/content/23/5/833

AJNR Am J Neuroradiol 23:833–837, May 2002

Case Report

Diffuse Metabolic Abnormalities in Reversible Posterior Leukoencephalopathy Syndrome

Florian S. Eichler, Paul Wang, Robert J. Wityk, Norman J. Beauchamp, Jr., and Peter B. Barker

Summary: Two cases of reversible posterior leukoencephalopathy syndrome were examined with proton MR spectroscopic imaging. Widespread metabolic abnormalities, consisting of increased choline and creatine levels and mildly decreased *N*-acetylaspartate, occurred in regions with both normal and abnormal MR imaging appearances. In one case for which proton MR spectroscopic imaging follow-up was available, all metabolite levels had returned to normal by 2 months. Proton MR spectroscopic imaging may be helpful for the diagnosis and investigation of the underlying pathophysiology of reversible posterior leukoencephalopathy syndrome.

The term *reversible posterior leukoencephalopathy syndrome* (RPLS) describes a syndrome of headaches, confusion, seizures, and visual disturbances associated with transient, predominantly posterior cerebral lesions revealed by neuroimaging (1). Because MR imaging (in particular, fluid-attenuated inversion recovery MR imaging) has shown that lesions can occur in both gray and white matter, the term *posterior reversible encephalopathy syndrome* has also been suggested (2). RPLS occurs in association with hypertension and/or immunosuppression (3), and known triggers include acute renal failure, eclampsia (especially puerperal), and the use of cyclosporine, FK506, or interferon-α (1). Considering that the list of causes of RPLS is growing (4–6), more information is needed regarding the underlying pathophysiology of this transient disorder. It is also clinically important to be able to distinguish RPLS from other disorders that may involve irreversible brain lesions.

The techniques of proton MR spectroscopy and MR spectroscopic imaging allow the in vivo measurement of various neurochemicals, which can provide information regarding the metabolism, cellular composition, and pathophysiology of brain lesions (7). Only isolated reports of MR spectroscopy of RPLS have been published (8–11). We herein report the findings of quantitative, multi-section proton MR spectroscopic imaging of two patients with RPLS.

Received November 14, 2001; accepted after revision December 7.

From the Department of Neurogenetics (F.S.E.), Kennedy Krieger Institute, and the Departments of Radiology (P.W., N.J.B., P.B.B.) and Neurology (R.J.W.), The Johns Hopkins University, Baltimore, MD.

Address reprint requests to Peter B. Barker, PhD, Department of Radiology, MRI 143C, The Johns Hopkins University School of Medicine, 600 N. Wolfe Street, Baltimore, MD 21287.

Proton MR Spectroscopic Imaging

All imaging was performed at 1.5 T. Four oblique axial sections (section thickness, 15 mm; intersection gap, 2.5 mm) were obtained parallel to the anterior commissure-posterior commissure line for proton MR spectroscopic imaging (2300/272 [TR/TE]; field of view, 24 cm; matrix size, 32 × 32; one signal average). Outer volume saturation pulses were used for suppression of lipid and water signals originating from the skull and scalp, and a chemical shift-selective saturation pulse was used for water suppression. The nominal voxel size was 0.8 cm^3. Full technical details are provided elsewhere (12). MR spectroscopic imaging data were processed as previously described (13). Metabolite peak areas were measured using a simplex routine, assuming gaussian line shapes. Concentrations of *N*-acetylaspartate, creatine, and choline were estimated by the phantom replacement technique (14). Voxels were analyzed in the occipital white and gray matter, the centrum semiovale, and insular gray matter and were compared with published normal values (13, 14). Patient 1 was evaluated with MR spectroscopic imaging during the episode only. For patient 2, MR spectroscopic imaging was performed both during the episode and at follow-up 2 months later. Metabolite levels were compared between the episode and follow-up findings by using the Mann-Whitney nonparametric test.

Patient 1

The MR images of a 38-year-old woman with acute myelomonocytic leukemia showed leptomeningeal enhancement after induction of chemotherapy. Because of concern regarding CSF seeding, intrathecal cytarabine with subsequent consolidation with high dose (6 g) cytarabine was IV administered. Because of development of multi-organ sepsis, the patient was monitored in the intensive care unit for hypertensive crisis (blood pressure, 180/80 mmHg) and lowered consciousness. She was observed to have a seizure and was unresponsive, with a dilated left pupil.

T2-weighted and fluid-attenuated inversion recovery MR images showed bilateral areas of signal hyperintensity in the posterior white and gray matter, with extension into the frontal lobe in the left hemisphere (Fig 1A and B). Sparing of calcarine and paramedian occipital lobe structures was noted, and no abnormalities were observed in the basal ganglia, brain stem, or cerebellum. Isotropic apparent diffusion coefficiency maps showed an increased diffusion constant (lesion apparent diffusion coefficiency, 1.56×10^{-3} mm^2/s; normal appearing brain, 0.85×10^{-3} mm^2/s) in the same distribution as that seen on fluid-attenuated inversion recovery MR images, whereas on diffusion-weighted images, the lesion was isointense to slightly hyperintense because of the opposing effects of T2 weighting (hyperintense) and diffusion weighting (hypointense) (15).

Figure 1, A and B, shows two MR spectroscopic imaging sections and selected spectra obtained during the episode. The ratios of *N*-acetylaspartate:choline and *N*-acetylaspartate:creatine were low, both in regions of the brain with normal and abnormal MR imaging appearance and in gray and white matter. Inspection of metabolic images suggests that metabolite levels were lower in the edematous regions of the brain, presumably a dilution effect reflecting the increased water content.

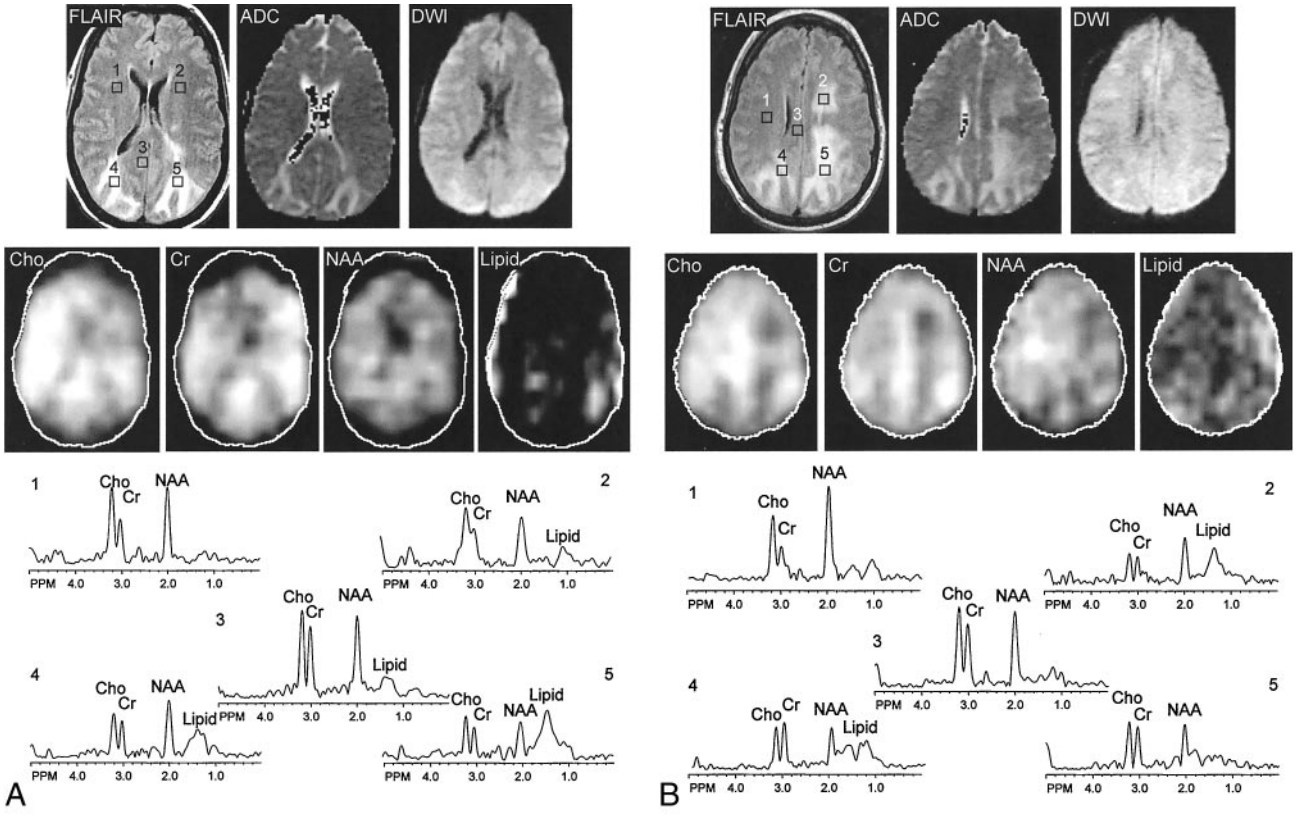

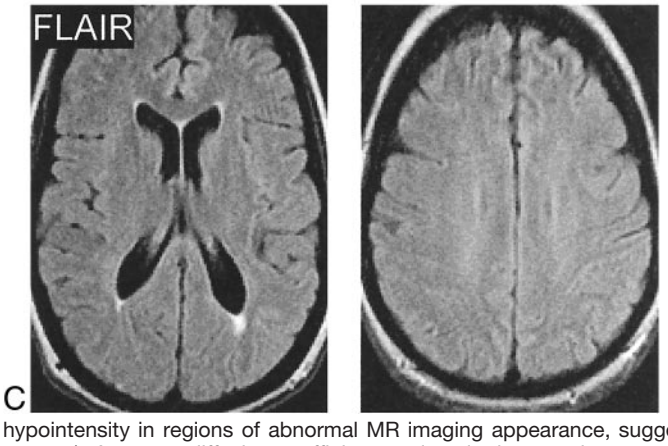

FIG 1. Patient 1. Fluid-attenuated inversion recovery (*FLAIR*) MR images, apparent diffusion coefficiency (*ADC*) maps, diffusion-weighted images (*DWI*), metabolic choline (*Cho*), creatine (*Cr*), *N*-acetylaspartate (*NAA*) and lipid images, and spectra are shown.

A, Images from the second of four MR spectroscopic imaging sections. Spectra are shown from selected regions of interest in frontal white matter, mesial occipital gray matter, and occipital white matter with fluid-attenuated inversion recovery MR imaging hyperintensity.

B, Images from the third of four MR spectroscopic imaging sections. Spectra are shown from frontal white matter, with both normal (*right*) and abnormal (*left*) MR imaging appearance, body of the corpus callosum, and parietal white matter with fluid-attenuated inversion recovery MR imaging hyperintensity. High levels of creatine and choline and mildly reduced *N*-acetylaspartate are apparent in both gray and white matter regions with normal MR imaging appearance. Lipid signals most likely result from head motion. Metabolic images show hypointensity in regions of abnormal MR imaging appearance, suggesting dilution of all metabolite concentrations (increased water content). Apparent diffusion coefficiency values in these regions are also elevated compared with normal values.

C, Fluid-attenuated inversion recovery MR images, obtained at 2-month follow-up, show normalization of signal intensity with only a small region of fluid-attenuated inversion recovery MR imaging hyperintensity adjacent to the posterior horns of the lateral ventricles.

Some signals in the 1.0- to 1.5-ppm region of the spectrum were also observed and were attributable to lipids, but these did not localize well to either specific brain locations or lesions and therefore seem most likely to be the result of mild head motion, which "smears" the intense lipid signals throughout the phase-encoding directions. Quantitation of proton MR spectroscopic imaging (Table) indicates that the low ratios of *N*-acetylaspartate:choline and *N*-acetylaspartate:creatine are predominantly due to increased choline and creatine levels compared with normal values (typical normal values: choline, 1–2 mM; creatine, 5–7 mM; *N*-acetylaspartate, 7–13 mM depending on age, location, and measurement methodology) (13, 14).

The elevated blood pressure was treated with nitrates, esmolol, and mannitol. The patient's mental status remained abnormal, with waxing and waning disorientation. She complained of "blurry vision," headaches, and eye pain. Three days later, she again became acutely unresponsive with respiratory failure and required intubation. Her blood pressure was elevated at 140/90 mmHg, and her serum magnesium level had dropped to 0.9 mg/dL. She received phenytoin, nifedipine, and magnesium sulfate. Her status improved greatly, with extubation possible the next day. After extubation, a neuro-ophthalmologic examination documented cortical blindness, which slowly resolved during the next week. Subsequent magnesium levels ranged from 1.2 to 1.7 mg/dL (normal range, 1.3–2.0 mg/dL).

Follow-up MR imaging was performed 2 months after the initial episode, at which time the patient's condition was clinically normal (Fig 1C). MR imaging findings were normal, with the exception of some residual abnormal signal around the

Mean metabolite concentrations (mM, mean ± SD)

		Occipital WM	Centrum Semiovale	Occipital GM	Insular GM
Patient 1 (episode)	Cho	2.6 ± 0.8	2.8 ± 0.8	2.2 ± 0.6	2.9 ± 1.1
	Cr	8.4 ± 2.2	7.4 ± 2.0	7.1 ± 1.2	7.6 ± 2.3
	NAA	6.9 ± 1.9	6.8 ± 1.7	5.2 ± 1.3	6.0 ± 3.0
Patient 2 (episode)	Cho	3.3 ± 0.4*	3.7 ± 0.3*	2.7 ± 0.6*	3.2 ± 0.5*
	Cr	6.8 ± 1.8	8.2 ± 1.6*	7.9 ± 1.5*	7.9 ± 1.2*
	NAA	6.3 ± 0.8*	7.1 ± 0.7*	6.0 ± 1.5	6.1 ± 0.6
Patient 2 (follow-up)	Cho	2.1 ± 0.3	2.3 ± 0.3	1.6 ± 0.4	1.7 ± 0.5
	Cr	6.6 ± 1.4	6.9 ± 1.2	6.4 ± 1.4	6.3 ± 1.2
	NAA	7.9 ± 0.7	7.9 ± 0.3	6.8 ± 1.1	6.2 ± 0.8

Note.—WM indicates white matter; GM, gray matter; Cho, choline; Cr, creatine; NAA, *N*-acetylaspartate.
* $P < .05$ for comparison of values during episode and at follow-up (Mann-Whitney Nonparametric Test).

posterior horns of the lateral ventricles. Intrathecal therapy (consolidation) resumed 10 days after the last seizure. A total of four subsequent doses of intrathecal chemotherapy were administered without incident. The patient remained seizure-free, and phenytoin was discontinued after 3 months.

Patient 2

A 36-year-old primigravida with a diagnosis of acute pancreatitis underwent an emergency caesarian section at gestation of 36 weeks. Her pancreatitis was complicated by fever and cholecystitis. She was placed on hemodialysis and total parenteral nutrition and subsequently developed acute renal failure. Two weeks after delivery, she experienced a generalized seizure and then persistent change in mental status. Blood pressure before her seizure was 180/90 mmHg, and subsequent blood pressures ranged from 160/80 to 180/100 mmHg. Spin-echo and T2-weighted MR images showed bilateral parieto-occipital signal hyperintensity (Fig 2A) involving both white and gray matter. A small amount of T2 hyperintensity was also noted in the subcortical white matter of the frontal lobe and cerebellum in the vicinity of the dentate nuclei. As for patient 1, MR spectroscopic imaging showed globally reduced ratios of *N*-acetylaspartate:choline and *N*-acetylaspartate:creatine, with choline especially high in the white matter with normal MR imaging appearance. Again, quantitative analysis (Table) revealed high levels of creatine and choline and mildly reduced *N*-acetylaspartate during the episode. Regions with MR T2 hyperintensity also showed lower levels of all metabolites, consistent with increased water content.

The seizures were treated with Ativan, and the blood pressure was controlled with labetolol and angiotensen-converting enzyme inhibitors. Daily serum magnesium levels ranged from 1.9 to 2.1 mg/dL. Follow-up MR imaging findings, obtained 2 months later when the patient showed clinical improvement, were normal (Fig 2B). Metabolite concentrations also recovered to near normal levels throughout the brain ($P < .05$ compared with episode levels) (Table 1). The patient remained seizure-free, and Ativan was discontinued after 3 months.

Discussion

Descriptions of RPLS have emphasized characteristic clinical and radiologic presentations despite the heterogeneous settings in which this transient syndrome occurs (1). Clinically, patients present with altered mental status, headaches, seizures, and visual disturbances. Hypertension is commonly associated with RPLS but may be relatively mild and is not universally present, especially in the setting of immunosuppression (16). Neuroimaging reveals the posterior parts of the cerebrum, especially the parieto-occipital regions, to be generally involved, with relative sparing of the occipital cortical gray matter (1).

The underlying pathophysiology of RPLS is not well understood, but two main mechanisms have been suggested (17). One hypothesis is that cerebral vasospasm results in ischemia and subsequent development of T2 hyperintensity (18–21). Alternatively, it has been suggested that there is a temporary failure of the autoregulatory capabilities of the cerebral vessels, leading to hyperperfusion, breakdown of the blood-brain barrier, and consequent vasogenic edema (5, 16, 22). Although there have been isolated reports of increased lactate signals (suggestive of ischemia) in individual patients with RPLS (8, 11), we did not identify any lactate signals in our two cases and the majority of cases presented in the literature also do not report elevated lactate (8–11). Diffusion MR imaging has also virtually ubiquitously shown elevated diffusion constants in cases of RPLS (as was seen in patient 1 here), again consistent with vasogenic edema and the absence of acute ischemic changes (16, 23, 24).

The preferential involvement of the parietal and occipital lobes is thought to be related to the relatively poor sympathetic innervation of the posterior circulation (1, 25). Presumably, this hyperperfusion is triggered by hypertension (25). Drugs have been postulated to contribute to this physiological effect, by cytotoxic effects on the vascular endothelium or by inducing or exacerbating hypertension (1, 16).

In both cases reported herein, proton MR spectroscopic imaging showed diffuse metabolic abnormalities (increases in both choline and creatine and mildly reduced *N*-acetylaspartate) in both white and gray matter throughout the brain (ie, including areas that were of normal T2 or fluid-attenuated inversion recovery MR imaging appearance and had normal apparent diffusion coefficiency). Follow-up of patient 2 revealed that these abnormalities had resolved, with near normal levels of all metabolites. Previous MR spectroscopy studies of RPLS have generally used nonquantitative single voxel techniques that did not examine brain regions with normal MR imaging appearance, but spectra from lesions have been re-

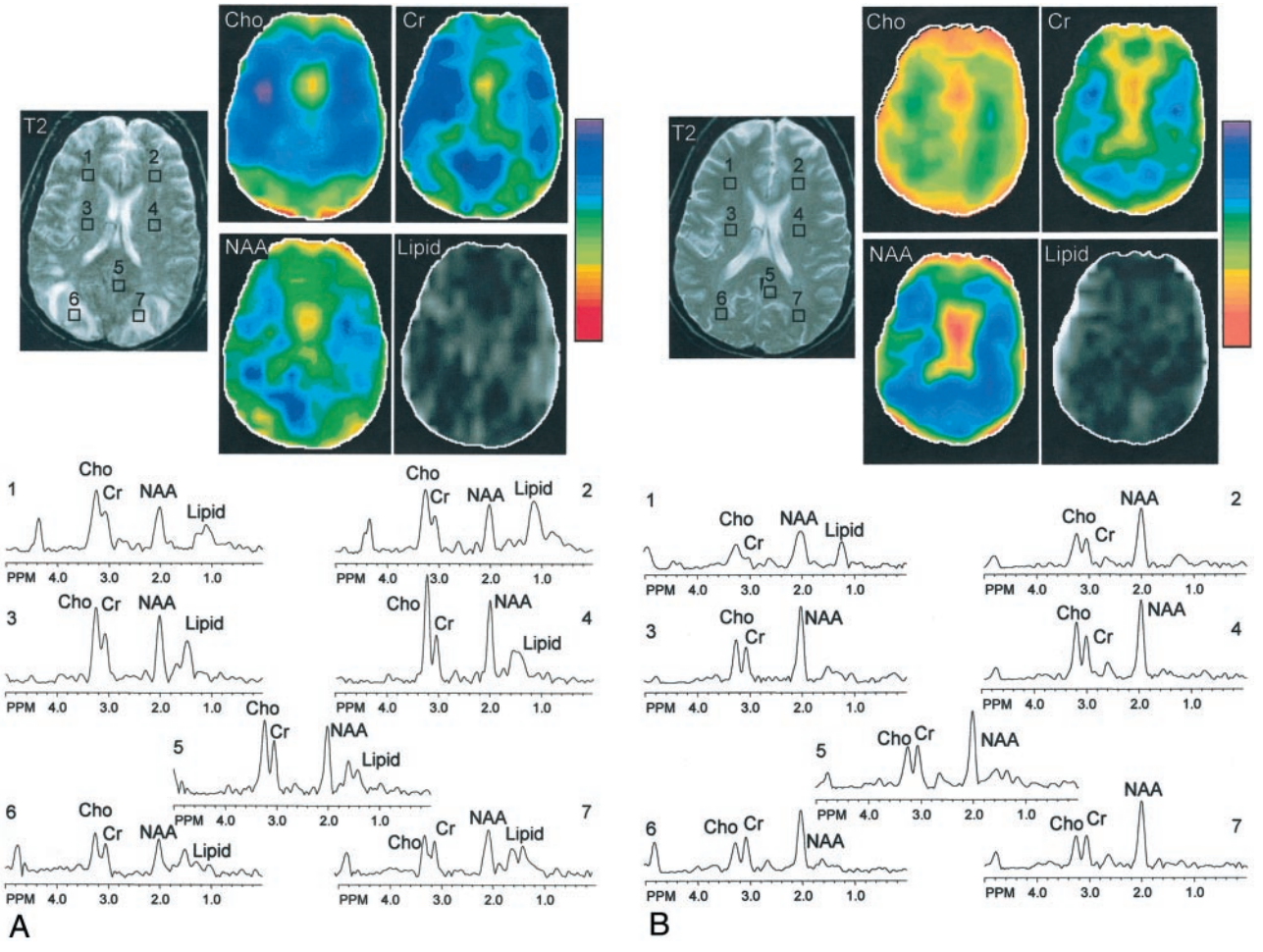

FIG 2. Patient 2. T2-weighted MR images, metabolic choline (*Cho*), creatine (*Cr*), *N*-acetylaspartate (*NAA*), and lipid images, and spectra from selected regions of interest (frontal and posterior white matter, mesial occipital gray matter) are shown.

A, Images obtained at time of episode. Quantitative analysis (Table) indicated that the primary abnormality was increased levels of choline and creatine with mildly lower *N*-acetylaspartate.

B, Images obtained at 2-month follow-up. A globally reduced ratio of *N*-acetylaspartate:choline is apparent throughout the brain, which has normalized by the time of follow-up. As in Figure 1, posterior edematous regions exhibit lower signal intensity on MR spectroscopic images compared with other regions. MR spectroscopic imaging hypointensity in the frontal lobe (most noticeable in the creatine image) is an artifact due to magnetic field inhomogeneity in this region.

ported to have either normal (8, 10) or reduced (9, 11) ratios of *N*-acetylaspartate:creatine. The current study indicates that a diffuse, probably global, metabolic abnormality occurs in association with RPLS, even though the MR imaging manifestations are predominantly confined to posterior brain regions. The most pronounced change was an increase in choline (and, to a lesser extent, creatine) during the episode (Figs 1 and 2, Table 1). A rise in choline can have multiple causes, including increased membrane turnover, inflammation, demyelination, and increased glial cell density in proliferative processes (26, 27). However, the transient nature of the choline elevation, its global nature, and the reversibility of the MR imaging lesions limits the possible interpretations of the increase. Demyelination seems an unlikely cause because choline elevation was seen in both gray and white matter; histologic findings associated with eclampsia also do not support demyelination as an explanation (28). An alternative, perhaps more likely, explanation may be that the elevation of choline (and creatine) results from microglial activation; glial cells in vitro have been reported to have high levels of both choline and creatine (29). Pronounced microglial and astrocytic proliferation has been reported to occur after immunosuppressive measures, such as chemotherapy and radiation (30). Disruption of the blood-brain barrier and the presence of vasogenic edema could presumably result in the activation of microglial cells. However, this explanation must be regarded as speculative because histopathologic studies of RPLS are scarce and no evidence of microglial proliferation was found in postmortem cerebral lesions of patients with eclampsia in two reports (28, 31). Future studies of larger numbers of patients using other techniques are required to confirm or refute this hypothesis.

Concurrent with the rise in choline and creatine, a mildly reduced *N*-acetylaspartate signal was observed that normalized by the time of follow-up of patient 2. *N*-acetylaspartate is thought to be of neuronal/axonal origin in the mature brain (32), and its decrease could reflect decreased synthesis, increased use, or changes in

cellular density or composition (32). The reversible *N*-acetylaspartate reduction in the current study seems to be due to neuronal/axonal dysfunction secondary to microglial proliferation rather than permanent neuronal/axonal loss. It should also be noted that *N*-acetylaspartate was lower (as were creatine and choline) in regions with vasogenic edema, presumably reflecting a dilution effect secondary to increased water content.

Proton MR spectroscopic imaging may be useful in distinguishing RPLS from other focal lesions, such as infarction or demyelination, which may present with similar conventional MR imaging appearance. In cases of acute infarction, lactate would be expected to be elevated and apparent diffusion coefficiency reduced, neither of which was observed in the two cases presented herein. However, the relative ability of MR spectroscopic and diffusion-weighted imaging to distinguish RPLS from infarction is not known. Because apparent diffusion coefficiency may be normal or elevated in cases of subacute or chronic stroke, there may be some additional value for MR spectroscopic imaging compared with diffusion-weighted imaging in these cases. Active demyelination is usually associated with elevated choline and reduced *N*-acetylaspartate, similar to RPLS, but would not be expected to show the global gray and white matter metabolic changes that were observed in the two cases of RPLS presented herein.

In summary, we present two case reports of RPLS with marked, global metabolic abnormalities that were present in regions of the brain both with and without abnormal MR imaging appearance. These findings (increased choline and creatine, mildly decreased *N*-acetylaspartate) suggest a diffuse metabolic defect in association with RPLS, possibly consistent with microglial activation and neuronal dysfunction. These abnormalities were not predictive of poor neurologic outcome, and, in one patient who underwent follow-up MR spectroscopic imaging, were reversible.

Acknowledgments

We thank Drs. Jeffrey Duyn and Jan Willem van der Veen (National Institutes of Health, Bethesda, MD) for the MR spectroscopic imaging pulse sequence.

References

1. Hinchey J, Chaves C, Appignani B, et al. **A reversible posterior leukoencephalopathy syndrome.** *N Engl J Med* 1996;334:494–500
2. Casey SO, Sampaio RC, Michel E, Truwit CL. **Posterior reversible encephalopathy syndrome: utility of fluid-attenuated inversion recovery MR imaging in the detection of cortical and subcortical lesions.** *AJNR Am J Neuroradiol* 2000;21:1199–1206
3. Pavlakis SG, Frank Y, Chusid R. **Hypertensive encephalopathy, reversible occipitoparietal encephalopathy, or reversible posterior leukoencephalopathy: three names for an old syndrome.** *J Child Neurol* 1999;14:277–281
4. Delanty N, Vaughan C, Frucht S, Stubgen P. **Erythropoietin-associated hypertensive posterior leukoencephalopathy.** *Neurology* 1997;49:686–689
5. Ito Y, Arahata Y, Goto Y, et al. **Cisplatin neurotoxicity presenting as reversible posterior leukoencephalopathy syndrome.** *AJNR Am J Neuroradiol* 1998;19:415–417
6. Kupferschmidt H, Bont A, Schnorf H, et al. **Transient cortical blindness and bioccipital brain lesions in two patients with acute intermittent porphyria.** *Ann Intern Med* 1995;123:598–600
7. van Zijl PC, Barker PB. **Magnetic resonance spectroscopy and spectroscopic imaging for the study of brain metabolism.** In: Lester DS, Felder CC, Lewis EN, eds. *Imaging Brain Structure and Function*. New York: New York Academy of Science; 1997:75–96
8. Kwon S, Koo J, Lee S. **Clinical spectrum of reversible posterior leukoencephalopathy syndrome.** *Pediatr Neurol* 2001;24:361–364
9. Pavlakis SG, Frank Y, Kalina P, Chandra M, Lu D. **Occipital-parietal encephalopathy: a new name for an old syndrome.** *Pediatr Neurol* 1997;16:145–148
10. Russell MT, Nassif AS, Cacayorin ED, Awwad E, Perman W, Dunphy F. **Gemcitabine-associated posterior reversible encephalopathy syndrome: MR imaging and MR spectroscopy findings.** *Magn Reson Imaging* 2001;19:129–132
11. Sengar AR, Gupta RK, Dhanuka AK, Roy R, Das K. **MR imaging, MR angiography, and MR spectroscopy of the brain in eclampsia.** *AJNR Am J Neuroradiol* 1997;18:1485–1490
12. Duyn JH, Gillen J, Sobering G, van Zijl PC, Moonen CT. **Multisection proton MR spectroscopic imaging of the brain.** *Radiology* 1993;188:277–282
13. Soher BJ, van Zijl PC, Duyn JH, Barker PB. **Quantitative proton spectroscopic imaging of the human brain.** *Magn Reson Med* 1996; 35:356–363
14. Barker PB, Szopinski K, Horska A. **Metabolic heterogeneity at the level of the anterior and posterior commissures.** *Magn Reson Med* 2000;43:348–354
15. Casey S. **"T2 washout": an explanation for normal diffusion-weighted images despite abnormal apparent diffusion coefficient maps.** *AJNR Am J Neuroradiol* 2001;22:1450–1451
16. Ay H, Buonanno FS, Schaefer PW, et al. **Posterior leukoencephalopathy without severe hypertension: utility of diffusion-weighted MRI.** *Neurology* 1998;51:1369–1376
17. Port JD, Beauchamp NJ Jr. **Reversible intracerebral pathologic entities mediated by vascular autoregulatory dysfunction.** *Radiographics* 1998;18:353–367
18. Horn EH, Filshie M, Kerslake RW, Jaspan T, Worthington BS, Rubin PC. **Widespread cerebral ischaemia treated with nimodipine in a patient with eclampsia.** *BMJ* 1990;301:794
19. Ito T, Sakai T, Inagawa S, Utsu M, Bun T. **MR angiography of cerebral vasospasm in preeclampsia.** *AJNR Am J Neuroradiol* 1995; 16:1344–1346
20. Lewis LK, Hinshaw DB Jr, Will AD, Hasso AN, Thompson JR. **CT and angiographic correlation of severe neurological disease in toxemia of pregnancy.** *Neuroradiology* 1988;30:59–64
21. Trommer BL, Homer D, Mikhael MA. **Cerebral vasospasm and eclampsia.** *Stroke* 1988;19:326–329
22. Hauser RA, Lacey DM, Knight MR. **Hypertensive encephalopathy: magnetic resonance imaging demonstration of reversible cortical and white matter lesions.** *Arch Neurol* 1988;45:1078–1083
23. Mukherjee P, McKinstry RC. **Reversible posterior leukoencephalopathy syndrome: evaluation with diffusion-tensor MR imaging.** *Radiology* 2001;219:756–765
24. Provenzale JM, Petrella JR, Cruz LC Jr, Wong JC, Engelter S, Barboriak DP. **Quantitative assessment of diffusion abnormalities in posterior reversible encephalopathy syndrome.** *AJNR Am J Neuroradiol* 2001;22:1455–1461
25. Dillon WP, Rowley H. **The reversible posterior cerebral edema syndrome.** *AJNR Am J Neuroradiol* 1998;19:591
26. Bitsch A, Bruhn H, Vougioukas V, et al. **Inflammatory CNS demyelination: histopathologic correlation with in vivo quantitative proton MR spectroscopy.** *AJNR Am J Neuroradiol* 1999;20:1619–1627
27. Brenner RE, Munro PM, Williams SC, et al. **The proton NMR spectrum in acute EAE: the significance of the change in the Cho:Cr ratio.** *Magn Reson Med* 1993;29:737–745
28. Lindheimer MD, Roberts JM, Cunningham FG. *Chesley's Hypertensive Disorders in Pregnancy.* New York: McGraw Hill; 1999
29. Urenjak J, Williams SR, Gadian DG, Noble M. **Proton nuclear magnetic resonance spectroscopy unambiguously identifies different neural cell types.** *J Neurosci* 1993;13:981–989
30. van der Knaap MS, Valk J. **Leukoencephalopathy after chemotherapy and/or radiation.** In: van der Knaap MS, Valk J, eds. *Magnetic Resonance of Myelin, Myelination, and Myelin Disorders*. Berlin: Springer-Verlag; 1995:406–411
31. MacGillivray I. *Pre-Eclampsia: The Hypertensive Disease of Pregnancy.* Philadelphia: W.B Saunders Co.; 1983
32. Barker PB. ***N*-Acetylaspartate: a neuronal marker?** *Ann Neurol* 2001;49:423–424